Proceedings of the ASME 2008 International Design Engineering Technical Conferences & Computers and Information in Engineering Conference
IDETC/CIE 2008
August 3-6, 2008, Brooklyn, New York, USA

DETC2008-49550

MOBILITY AND GEOMETRICAL ANALYSIS OF A TWO ACTUATED SPOKE WHEEL ROBOT MODELED AS A MECHANISM WITH VARIABLE TOPOLOGY

Ya Wang
RoMeLa: Robotics & Mechanisms Laboratory
Mechanical Engineering Department
Virginia Polytechnic and State University
Blacksburg, Virginia 24061
Email: ywang07@vt.edu

Ping Ren
RoMeLa: Robotics & Mechanisms Laboratory
Mechanical Engineering Department
Virginia Polytechnic and State University
Blacksburg, Virginia 24061
Email: renping@vt.edu

Dennis Hong[1]
RoMeLa: Robotics & Mechanisms Laboratory
Mechanical Engineering Department
Virginia Polytechnic and State University
Blacksburg, Virginia 24061
Email: dhong@vt.edu

ABSTRACT

In this paper, the mobility and geometrical analysis of a novel mobile robot that utilizes two actuated spoke wheels is presented. Intelligent Mobility Platform with Active Spoke System (IMPASS) is a wheel-leg hybrid robot that can walk in unstructured environments by stretching in or out three independently actuated spokes of each wheel. First, the unique locomotion scheme of IMPASS is introduced and the definitions of the coordinate systems are developed to describe the kinematic configurations. Since this robot is capable of utilizing its metamorphic configurations to implement different types of motion, its topology structures are classified into different groups based on the cases of ground contact points. For each contact point case, the mobility analysis is performed using the conventional *Grübler* and *Kutzbach* criterion. However, as for the cases in which the structure is overconstrained, the Modified *Grübler* and *Kutzbach* criterion based on reciprocal screws are implemented to obtain the correct number of degrees of freedom. *Line geometry* is adopted to assist in the process. Additionally, the geometrical constraint equations of the robot are derived. The results in this work lay the foundation of the future research on inverse and forward kinematics, instantaneous kinematics, dynamics analysis and motion planning of this unique locomotion robot.

1.INTRODUCTION

Recently, leg-wheel hybrid robots have been drawing more attention since they have the advantages of both legs and wheels. The legged locomotion is more adaptable to a wide range of unstructured ground environments, while the wheeled locomotion is fast on smooth surfaces. However, the use of legs and wheels can be a good synthesis for a walking machine combining the merits of both locomotion types.

One particular application is the robot that combines the wheel and the leg in each limb. Usually, wheels are located at the end of each limb, which allows the robot to navigate as a rover or walk with legs when the wheel's rotation is locked, as demonstrated with ALDURO (the Anthropomorphically Legged and Wheeled Duisburg Robot), developed by Hiller and et. al. [1], as well as ATHLETE (All-Terrain Hex-Legged Extra-Terrestrial Explorer), designed by JPL (Jet Propulsion Laboratory) [2]. Another useful application is the robot that has both wheels and legs on separate limbs, like the hybrid robot proposed by Suwannasit and Laksanacharoen [3]. Moreover, Shores and Minor [4] developed a new hybrid robot which is designed like a wheel, embracing all the benefits of rolling, walking and climbing locomotion.

Within the classification of leg-wheel hybrid robots, there is a group which integrates legs into the wheels of the robot, creating a rimless spoke wheel. This greatly improves mobility, as can be seen in such robots as Scout [5, 6], RHex [7] and Whegs [8, 9]. The application of spokes not only improved the rough terrain mobility, but also increased the moving speed. Recently, RoMeLa (Robotics and Mechanisms Laboratory) at Virginia Tech proposed a novel high-mobility locomotion platform, called IMPASS (Intelligent Mobility Platform with Active Spoke System), as shown in Figure 1, which incorporates the benefits of wheeled, legged and spoke systems. IMPASS is designed to walk on various terrain, cross over obstacles, climb up steps, using the unique ability to intelligently stretch its spokes in or out. System design, kinematics modeling and preliminary analysis on motion

1. Address all correspondence to this author.

profiles, walking and turning states have been done in previous work [10-12].

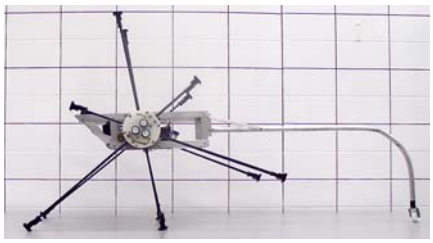

Figure 1. Prototype of IMPASS.

In this paper, the mobility and geometrical analysis of IMPASS is studied, which is the fundamental task of the inverse and forward position analysis, velocity analysis, error analysis, and dynamics analysis. The future goal of the mobility and geometrical analysis is to solve the position relationship between the moving platform and the ground contact points to perform a specific motion path.

The rest of the paper is organized as follows: in section 2, the system geometrical model of IMPASS is defined, and the system parameters, coordinates definitions, as well as model assumptions are also depicted. Then in section 3, the contact point cases are classified, and then conventional *Grübler* and *Kutzbach criterion* is used to perform mobility analysis case by case using. As for the cases under which the structure is overconstrained, the Modified *Grübler* and *Kutzbach criterion* using reciprocal screws are implemented to obtain the correct number of degrees of freedom. *Line geometry* is adopted to assist in the process. In section 4, geometrical constraints analysis, and calculation of spoke length are presented. At the end, in section 5, conclusions and future work are presented.

2.SYSTEM MODEL DEFINITION

As we saw in the prototype (Figure 1), IMPASS is designed with two actuated spoke wheels, connected through the axle, and a passive tail. The tail is designed to improve the stability and balance of IMPASS. Since it doesn't affect the mobility and geometrical analysis, it is not considered in this paper for simplicity. Each of the wheels is composed of three independently actuated spokes S_{1R} S_{4R}, S_{2R} S_{5R}, S_{3R} S_{6R}, and S_{1L} S_{4L}, S_{2L} S_{5L}, S_{3L} S_{6L}, which pass through the hub centers C_R and C_L, locating at each end of the axle (the *moving platform*), as shown in Figure 2.

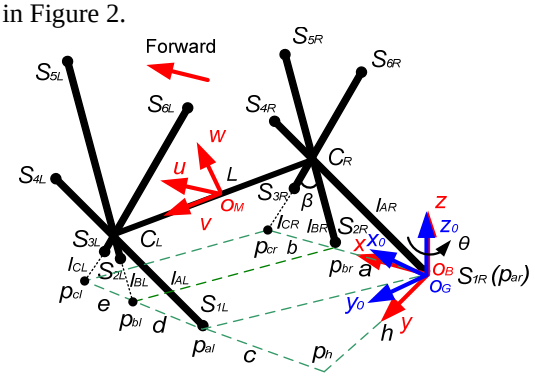

Figure 2. System Definition.

In order to describe the system geometrical model clearly, the system parameters and coordinates are defined as follows, which are also described in Table 1:

(1) The actual contact points (if the spokes are touching the ground) or projected contact points (if the spokes have not touched the ground) are numbered in sequence along the forward direction, from p_{ar}, p_{br} to p_{cr} of the right wheel and from p_{al}, p_{bl} to p_{cl} of the left wheel. For example, in Figure 1, p_{cr}, p_{bl} and p_{cl} are projected contact points.

(2) Effective lengths l_{AR} and l_{AL} represent the distances from the hub centers C_R and C_L to the first contact or projected contact points p_{ar} and p_{al}, respectively, which are called effective spoke lengths. Lengths l_{BR}, l_{BL}, l_{CR} and l_{CL}, are corresponding to the effective spoke lengths from the hub centers C_R and C_L to the next contact or projected contact points p_{br}, p_{bl}, p_{cr}, and p_{cl}.

(3) L refers to the length of the axle, l corresponds to the full length of each single spoke, R is defined as the effective spoke length ratio between the right spoke and the left spoke (e.g. the ratio between l_{AR} and l_{AL}), and β is defined as the angle between the neighboring spokes of the same wheel, which is fixed at 60°.

(4) The body Cartesian coordinate B (o_B, x, y, z) is attached to the first ground contact point p_{ar}. The origin o_B coincides with p_{ar}. The positive direction of x-axis points in the forward orientation of IMPASS, along the intersection between the right wheel plane and the ground. The z-axis is normal to the ground and points upward. In this paper, for convenience, we assume that the body Cartesian coordinate B only has the yaw angle θ, rotating with the global Cartesian coordinate G (o_G, x_0, y_0, z_0).

(5) The contact point coordinates in Body coordinate are denoted as: $p_{ar}(0,0,0)$, $p_{br}(a,0,0)$, $p_{cr}(b,0,0)$, $p_{al}(c,h,0)$, $p_{bl}(d,h,0)$ and $p_{cl}(e,h,0)$.

(6) The moving Cartesian coordinate M (o_M, u, v, w) is attached to the axle. The origin o_M is situated to the midpoint of the axle. The u-axis points along the forward direction, and v-axis is located along the axle from C_R to C_L, as illustrated in Figure 2.

(7) Based on if the right/left (effective) length ratio R is always equal to 1, the system is analyzed as 3D Spatial ($R \neq 1$) or 2D ($R = 1$) Planar model. The latter has been discussed in detail in [10].

In this paper, the following assumptions have been made:

(1) The spokes and the axle are stiff.

(2) Two actuated spoke wheels are considered to be driven by a single axle, which is consistently perpendicular to each spoke. Therefore, the left wheel always has the same phase angle as the right wheel.

(3) All spokes have the same length and every right spoke has one corresponding parallel left spoke.

(4) The ground is assumed to be flat, so that all the ground contact points are always in the same plane.

(5) As the IMPASS walks, no slip and no bounce occur at the ground- contact points.

(6) The tail in Figure 1 is not considered.

Table 1. Nomenclature

Symbol	Definition
S_{1R} S_{4R}, S_{2R} S_{5R}, S_{3R} S_{6R}	Three spokes on right wheel
S_{1L} S_{4L}, S_{2L} S_{5L}, S_{3L} S_{6L}	Three spokes on left wheel
C_R , C_L	Hub centers on both ends of axle
p_{ar}, p_{br}, p_{cr}	Actual/Projected contact points in right wheel
p_{al}, p_{bl}, p_{cl}	Actual/Projected contact points in left wheel
l_{AR},l_{BR},l_{CR}	Effective right spoke length
l_{AL},l_{BL},l_{CL}	Effective left spoke length
L	Length of the axle
l	Full length of each spoke
β (60°)	Angle of neighboring spokes
R	Right /left effective spoke length ratio
B (o_B, x, y, z)	Body Cartesian coordinate
G (o_G, x_0 , y_0 , z_0)	Global Cartesian coordinate
M (o_M, u, v, w)	Moving Cartesian coordinate
θ	Yaw angle of body coordinate B about global coordinate G
p_{ar}(0,0,0), p_{br}(a,0,0), p_{cr}(b,0,0), p_{al}(c,h,0), p_{bl} (d,h,0),p_{cl}(e,h,0)	Contact points coordinates in body coordinate B

3. MOBILITY ANALYSIS

Since in each wheel there are three spokes that can be independently actuated at one time, the wheel can have one, two, or at most three contact points with the ground. Given the fact that the proposed prototype of IMPASS has two wheels, the combinations of possible cases of contact points in left and right wheels constitute the complete group of the topology structures of the robot. The robot can be considered as a mechanism with variable topologies (MVT). Unlike the "kinematoropic linkages" proposed firstly by Wohlhart in [13] which changes its permanent finite mobility through joint variables, and the "metamorphic mechanisms" originated by Dai and Jones in [14] which changes its mobility through the combinations of the kinematic links, this robot changes its mobility through the schemes of adjacency between its spokes (treated as prismatic joints) and the ground (treated usually as Link 0 in kinematic analysis). Through this point of view, the motions of straight-line walking, steady state turning and transient turning of this robot which are sufficiently discussed in [10-12] can be treated as the "metamorphing" of the mechanism from one configuration to another. Since the characteristics of the mobility in various topology structures are very different, a complete study on the mobility of all possible configurations of this robot is quite necessary.

Usually, the well-known *Grübler* and *Kutzbach criterion* is used to analyze the mobility of mechanisms, which is written as [15]:

$$M = d(n - g - 1) + \sum_{i=1}^{g} f_i - \zeta \quad (1)$$

where n is the number of links, g the number of joints, and f_i the d.o.f. of joint i, ζ is the number of passive d.o.f., d is taken as 3 for planar mechanisms and 6 for spatial mechanisms.

However, classical *Grübler* and *Kutzbach criterion* cannot reach the correct result of the mobility when it is applied directly to overconstrained mechanisms. Tsai and Stamper's University of Maryland manipulator is a famous example of such mechanisms [16]. The topology of those mechanisms often features multiple limbs and parallel structures. Due to the special arrangement of the links and joints, many of the constraints imposed by the limbs are redundant. Previous research on the mobility analysis of overconstrained mechanisms includes [17] and [18]. Most recently, a modified *Grübler* and *Kutzbach criterion* using reciprocal screws is proposed by Huang and Ge in [19], which offers a simple and direct method to solve the problem:

$$M = d(n - g - 1) + \sum_{i=1}^{g} f_i + \nu - \zeta \quad (2)$$

The definitions of most of the terms in Eq.(2) are the same as those in Eq.(1). The difference is the definition of d and the additional correction term ν . Here, d is given by:

$$d = 6 - \lambda \quad (3)$$

which is the order of the mechanism. λ is the number of the common constraints, which is defined as the common reciprocal screws of all limbs in a parallel mechanism [19]. ν is the number of redundant constrains or passive constraints which frequently appear when multiple limbs are connected to form the parallel mechanisms. The expression of ν is shown in the following equation:

$$\nu = \sum_{1}^{p} q_i - \lambda \quad p - k \quad (4)$$

where p is the number of limbs of the mechanism, q_i the number of constraint screws imposed by the i^{th} limb and k is the number of linearly independent constrains in the linear space of the constraint screws imposed by all limbs. The theoretical elucidation of this method can be founded in [20].

Mobility analysis on various topology structures of IMPASS is the focus of this section. These structures are classified based on different cases of actual contact points and *Grübler Kutzbach criterion* is utilized to calculate the number of d.o.f for each case. For those overconstrained configurations under which the classical mobility criterion fail, the Modified *Grübler* and *Kutzbach criterion* is adopted to reach the correct result.

Note that, in order to clarify the mobility analysis as conveniently as possible and without losing generality, the terminology n_1-n_2 is used to represent each case of contact points. In the following figures, the red arrow stands for the forward of the robot. With respect of this forward direction, n_1 denotes the number of actual contact points in the right spoke wheel while n_2 stands for the number of actual contact points

in the left spoke wheel. All cases of contact points are divided into three groups (1-*i*, 2-*j*, 3-*r*) in an enumerative manner, with i = 0, 1, j = 0, 1, 2, and r = 0,1,2,3. These contact points are usually treated as spherical joints with three d.o.f. in kinematic analysis. In summary, the kinematics models of the robot with variable configurations are classified into three groups and twenty (4+10+6=20) cases totally based on various modes of ground contact points in left and right wheels. These cases as displayed in Table 2.

3.1 1-*i* contact cases:

1-*i* contact cases are classified in Group 1, which have 1 right contact points and 0 or 1 left contact points, with totally 4 different possibilities as demonstrated in Figure 3.

3.1.1 1-0 contact case:

An example of 1-0 case is shown in Figure 3 (a). The actual contact point can be any one of the six points. Using Eq.(1), the mobility then becomes:

$$M = 6(3 - 2 - 1) + (3 + 1) = 4 \qquad (5)$$

By inspection, the d.o.f of this configuration are very easy to identify. The contact point of the robot with the ground can be treated as a spherical joint. The spoke itself also has a translational d.o.f.. The robot in this configuration is actually a serial manipulator with 4 d.o.f.. However, this configuration is an uncontrollable mode because the spherical joint is completely passive.

Table 2. Contact Case Classification

Group	Class 1	Class 2
1-*i* (4)	1-0(1)	$p_{ar} - 0$
	1-1(3)	p_{ar}-p_{al} (Parallel)
		p_{ar}-p_{bl}, p_{ar}-p_{cl} (Skew)
2-*j*(10)	2-0(2)	$p_{ar}\,p_{br}$ - 0, $p_{ar}\,p_{cr} - 0$
	2-1(4)	$p_{ar}\,p_{br}$ - p_{al}, $p_{ar}\,p_{br}$ -p_{cl}, $p_{ar}\,p_{cr}$ -p_{al}, $p_{ar}\,p_{cr}$ - p_{bl}
	2-2(4)	$p_{ar}\,p_{br}$ - $p_{al}\,p_{bl}$, $p_{ar}\,p_{br}$ - $p_{bl}\,p_{cl}$, $p_{ar}\,p_{br}$ - $p_{al}\,p_{cl}$, $p_{ar}\,p_{cr}$ - $p_{al}\,p_{cl}$
3-*r*(6)	3-0(1)	$p_{ar}\,p_{br}\,p_{cr} - 0$
	3-1(2)	$p_{ar}\,p_{br}\,p_{cr}$ - p_{al}, $p_{ar}\,p_{br}\,p_{cr}$ -p_{bl}
	3-2(2)	$p_{ar}\,p_{br}\,p_{cr}$ - $p_{al}\,p_{bl}$, $p_{ar}\,p_{br}\,p_{cr}$ - $p_{al}\,p_{cl}$
	3-3(1)	$p_{ar}\,p_{br}\,p_{cr}$ - $p_{al}\,p_{bl}\,p_{cl}$

3.1.2 1-1 contact case:

This case has two sub-cases depending on either the right spoke is parallel to the left spoke or skew to it. These two cases are shown in Figure 3 (b) and (c) respectively. Note that, the skew case has two variants depending on the twisting angle between the two spokes. The mobility criterion of these cases is the same. Using Eq. (1), the mobility is:

$$M = 6(4 - 4 - 1) + (3 \times 2 + 1 \times 2) = 2 \qquad (6)$$

Among these two d.o.f., one d.o.f. is the rotation of the robot about the pivot line ($P_{ar}P_{bl}$, $P_{ar}P_{cl}$ in Figure 3(c)) on the ground which connects the two contact points. This d.o.f. can be controlled by changing the phase angle of the two spoke wheels. The other d.o.f. is caused by changing the lengths of the two spokes simultaneously. Since the two spokes in contact with the ground do not slip or bounce, the distance between the two contact points ($P_{ar}P_{bl}$, $P_{ar}P_{cl}$) is treated as a constant in these cases. The geometric relationship of the spoke lengths, the forward and inverse kinematic analysis of this two-limb SP parallel mechanism are studied in details in [23].

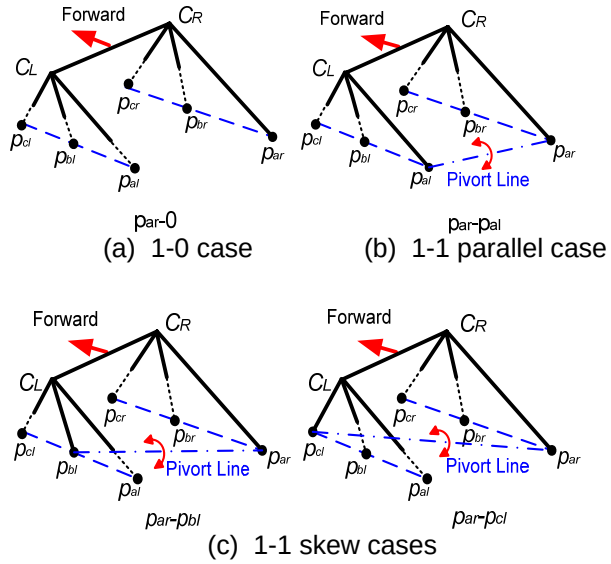

Figure 3. 1-*i* Contact Cases.

3.2 2-*j* contact cases:

Group 2 includes all possible 2-*j* contact cases which have 2 right contact points and 10 possibilities in total. Among these different cases, 2-0 has 2 sub-cases, 2-1 has 4 sub-cases and 2-2 has 4 sub-cases, as shown in Figure 4.

3.2.1 2-0 contact case:

In Figure 4 (a), two sub-cases of 2-0 occur when only two 60°or 120° spokes of the right wheel contact the ground. The mobility analysis using Eq. (1) yields:

$$M = 6(4 - 4 - 1) + (3 \times 2 + 1 \times 2) = 2 \qquad (7)$$

Again, these two d.o.f. can be easily identified by inspection. One d.o.f. is the rotation of the robot about the sideways pivot line ($P_{ar}P_{br}$, $P_{ar}P_{cr}$) on the ground connecting the two contact points. The other d.o.f. is pretty similar to the Two-point Contact Scheme discussed in [10] which is shown in Figure 5.

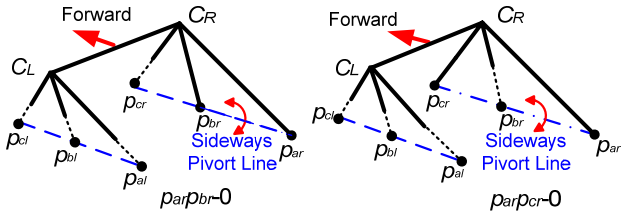

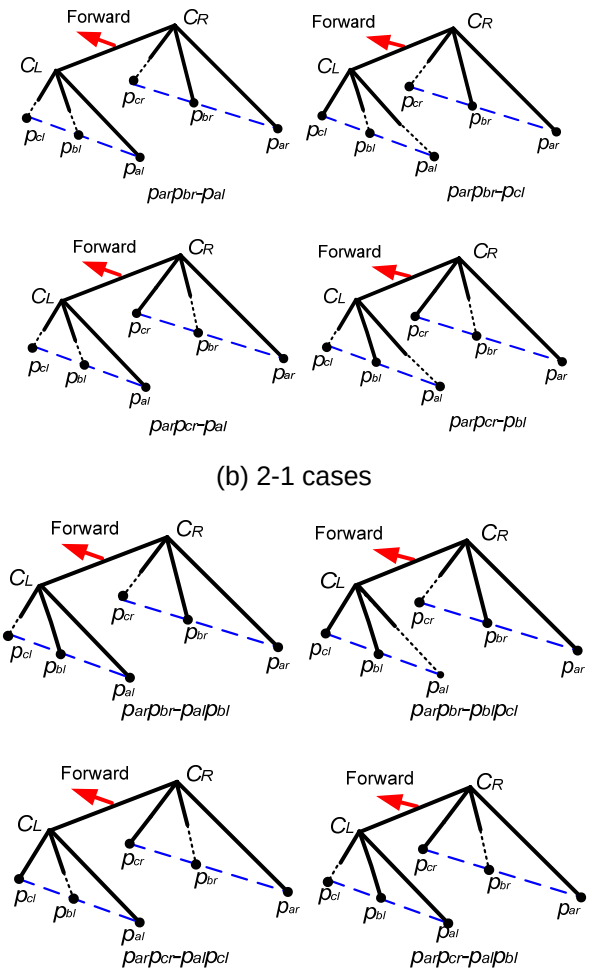

(b) 2-1 cases

(c) 2-2 cases

Figure 4. 2-*j* Contact Cases.

Due to no slip or bounce assumption, the distance between the two contact points ($P_{ar}P_{br}$, $P_{ar}P_{cr}$) is treated as a constant. The axle of the robot is constrained to move along an arc of a circle with the central angle of 120°C or 240°C (in Figure 5). Note that, the configurations in 2-0 cases are still the uncontrollable modes of the robot because the rotational d.o.f is completely passive.

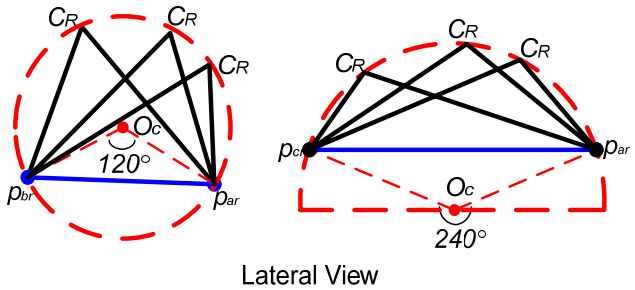

Lateral View

Figure 5. The Concept of the Two-Point Contact Scheme [10].

3.2.2 2-1 contact case:

As shown in Figure 4 (b), there are 4 sub-cases existing in the configurations of 2-1 contact point schemes. Note that, $p_{ar}p_{br}$-p_{al} and $p_{ar}p_{br}$-p_{bl} are treated as one sub-case; $p_{ar}p_{cr}$-p_{al} and $p_{ar}p_{cr}$-p_{cl} are treated as one sub-case and so are $p_{ar}p_{br}$-p_{cl} and $p_{br}p_{cr}$-p_{al}. The mobility analysis using the conventional criterion in Eq. (1) yields the following result:

$$M = 6(5-6-1)+(3\times 3+1\times 3)=0 \qquad (8)$$

According to this result, the configurations of the robot in 2-1 cases have zero d.o.f.. However, the zero mobility derived from Eq.(1) only holds true for the sub-cases of $p_{ar}p_{br}$-p_{cl} and $p_{ar}p_{cr}$-p_{bl}. As for the sub-cases of $p_{ar}p_{br}$-p_{al} and $p_{ar}p_{cr}$-p_{al}, the result of zero mobility is apparently incorrect when the two parallel spokes in contact with the ground are of equal lengths. The d.o.f of the robot in 2-1 cases when its two spokes are parallel has already been identified in [12], which is a planar motion similar to the Two-point Contact Scheme in [10].

In order to explain this conflict, the Modified *Grübler* and *Kutzbach criterion* in Eq.(2) is utilized. The following subsections will focus on the identification of the number of redundant constrains ν.

First, with the condition of no-slip and no-bounce, the robot with three spokes in contact with the ground is considered as a parallel mechanism with three limbs connecting the moving platform to the fixed base. Each spoke has a spherical joint with three d.o.f. and one prismatic joint with one d.o.f..

Then the Spherical-Prismatic dyad forms a screw system with order 4. Correspondingly, its reciprocal screw system forms a planar pencil with the center at the contact point and perpendicular to the limb. Detailed discussion of the reciprocal screws of kinematic chains can be found in [15]. Since a planar pencil is a line variety with the order of 2, the common constraints q_i in Eq.(4) is taken as 2. As shown in Figure 6, the three planar pencils at the three contact points form the constraint screw system of the SP parallel mechanism. Since there is no line existing that belongs to the three planar pencils simultaneously, the common constraint λ is taken as 0 and d equals 6 by Eq.(3).

Thirdly, k is the number of linearly independent screws in the constraint system which consists of three planar pencils. Since all the reciprocal screws in this particular case have zero pitch and can be treated as *Plücker line coordinates*, *Grassmann geometry*, also known as *line geometry*, is adopted to identify the value of k. Detailed introduction regarding line geometry and its application in robotics and computer-aided design can be found in [21] and [22]. Taking any two lines from each of the planar pencils $\boldsymbol{P_1}$, $\boldsymbol{P_2}$ and $\boldsymbol{P_3}$, as shown in Figure 6 (a) and (b), these six lines constitute a line variety denoted by Γ, and k is determined by checking the order of Γ.

Based on the conditions and assumptions above, Eq.(4) becomes:

$$\nu = 2\times 3-0\times 3-k=6-k \qquad (9)$$

The order of Γ is determined by inspection. As demonstrated in Figure 6 (a), if the two parallel spokes in the sub-cases of 2-1, i.e. $p_{ar}p_{br}$-p_{al} and $p_{ar}p_{cr}$-p_{al}, are of unequal length, then the three planar pencils $\boldsymbol{P_1}$, $\boldsymbol{P_2}$ and $\boldsymbol{P_3}$ are un-coplanar, thus forming a line variety of order 6. However if the two parallel spokes are of equal length as shown in Figure 6 (b), then $\boldsymbol{P_1}$ is coplanar with $\boldsymbol{P_3}$ on plane $\boldsymbol{N}$. By inspection, plane $\boldsymbol{N}$ has a common line with plane $\boldsymbol{M}$ where $\boldsymbol{P_2}$ lies. Therefore, all the six lines in Γ will definitely intersect this common line, which is represented with the blue line in the figure, thus forming a line variety called *special complex* with the order of only 5. As a brief summary, if k equals 6, then the additional term ν standing for redundant constraints disappears and the mobility by Eq.(2) is the same as that by Eq.(1). If k equals 5, then ν is equal to 1 by Eq.(9).

The mobility by Eq.(2) based on the result from Eq.(9) is 1, which shows that the correct number of d.o.f. is successfully identified by using the modified criterion.

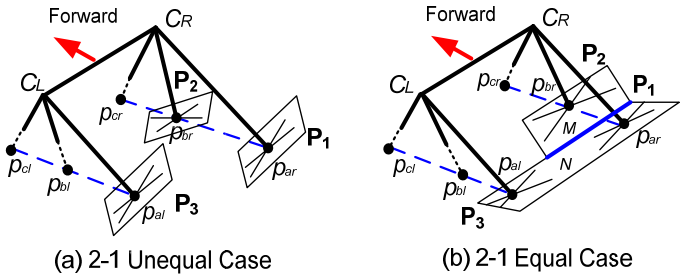

Figure 6. The Constraint Screw System of the 3-spoke SP Parallel Mechanism.

3.2.3 2-2 contact case:

Four types of 2-2 are displayed in Figure 4 (c). The mobility analysis based on Eq.(1) yields the following results:

$$M = 6(6-8-1)+(3\times 4+1\times 4) = -2 \qquad (10)$$

The negative number of d.o.f indicates that the robot is in an overconstrained configuration. An overconstrained mechanism sometimes has zero mobility but sometimes does possess finite d.o.f, such as University of Maryland manipulator [16]. As for the sub-cases of $p_{ar}p_{br}$-$p_{bl}p_{cl}$ and $p_{ar}p_{cr}$-$p_{al}p_{bl}$, the result of zero mobility is true. But for the sub-cases of $p_{ar}p_{br}$-$p_{al}p_{bl}$ and $p_{ar}p_{cr}$-$p_{al}p_{cl}$, similar to 2-1 cases, the d.o.f. of this four spokes SP parallel mechanism when each of the two pairs of parallel spokes is of the same length is not identified using Eq.(1). Eq.(2) has to be utilized again to deal with it.

As shown in Figure 7, each of the four spokes has a reciprocal screw system in the form of a planar pencil. Four planar pencils, $\boldsymbol{P_1}$, $\boldsymbol{P_2}$, $\boldsymbol{P_3}$ and $\boldsymbol{P_4}$, form the whole constraint system of the mechanism. Since no line exists that belongs to the four pencils simultaneously, λ is taken as 0. Take any two lines from each of the four pencils, thus forming a line variety Γ. In Figure 7 (a), if the lengths of the parallel spokes are not equal, then any two of the pencils are not coplanar. The order of Γ is 6. Eq.(4) yields:

$$\nu = 2\times 4-0\times 4-6 = 2 \qquad (11)$$

Substitute Eq.(11) back into Eq.(2), then

$$M = 6(6-8-1)+(3\times 4+1\times 4)+2 = -2+2 = 0 \qquad (12)$$

which shows the characteristic of zero mobility when the parallel spokes are not of equal length.

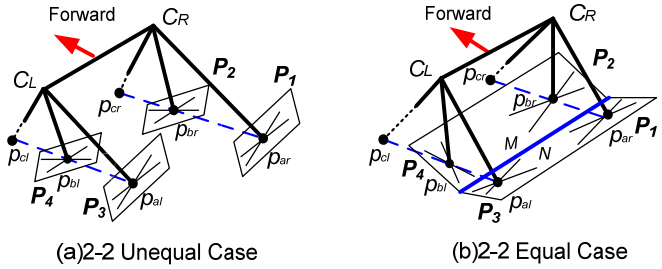

Figure 7. The Constraint Screw System of the 4-spoke SP Parallel Mechanism.

Figure 7 (b) shows the situation when the parallel spokes are equal. $\boldsymbol{P_2}$ is coplanar with $\boldsymbol{P_4}$ on plane $\boldsymbol{M}$ while $\boldsymbol{P_1}$ is coplanar with $\boldsymbol{P_3}$ on plane $\boldsymbol{N}$. By inspection, a common line of $\boldsymbol{M}$ and $\boldsymbol{N}$ exists that intersects all eight lines. Therefore, the line variety Γ formed by the eight lines is a *special complex* with the order of 5. The redundant constraint ν becomes:

$$\nu = 2\times 4-0\times 4-5 = 3 \qquad (13)$$

Using Eq.(2):

$$M = 6(6-8-1)+(3\times 4+1\times 4)+3 = -2+3 = 1 \qquad (14)$$

Therefore, the additional d.o.f. is identified. Again, this d.o.f. is similar to the Two-point Contact Scheme discussed in [10] given that the parallel spokes of the robot are always of the same length under this particular configuration. Note that, this d.o.f. can also be treated as a 2D planar motion when the mechanism is projected onto the plane which contains the spoke wheel. The 2D mobility analysis by Eq.(1) can be used to confirm the result in Eq.(10):

$$M = 3(4-4-1)+1\times 4 = 1 \qquad (15)$$

3.3 3-*r* contact cases:

3-*r* contact cases are in Group 3, which has 6 possibilities as illustrated in Figure 8.

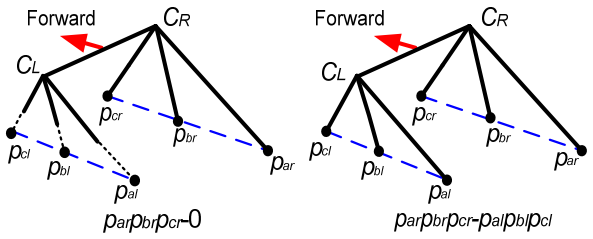

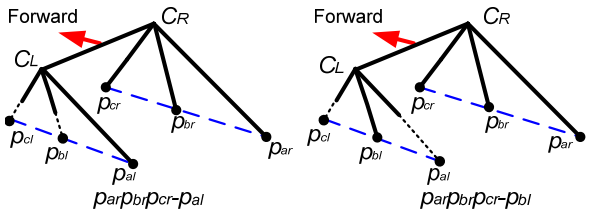

(c) 3-1 Cases

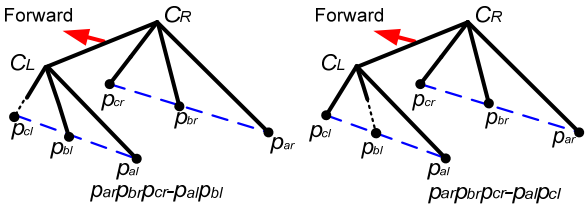

(d) 3-2 Cases

Figure 8. 3-*r* Contact Cases.

3.3.1 3-0 contact case:

If the conventional *Grübler* and *Kutzbach criterion* is used the derive the number of d.o.f. in 3-0 (Figure 8 (a)), then the parameters in Eq.(1) will take exactly the same value as those in Eq.(8). The zero mobility is obviously inaccurate, because by inspection, the body of the robot can definitely rotate about the line which connects all three contact points. By using the Modified criterion in Eq.(2), the correct number of d.o.f in this overconstrained mechanism can be obtained. The procedures are the same as 2-1 cases.

As shown in Figure 9 (a), three planar pencils $\boldsymbol{P_1}$, $\boldsymbol{P_2}$ and $\boldsymbol{P_3}$ form the constraint screw system the mechanism. Again, no line exists that belongs to $\boldsymbol{P_1}$, $\boldsymbol{P_2}$ and $\boldsymbol{P_3}$ at the same time, so λ is taken as 0. Take any two lines from each of the pencils; a line variety Γ with six lines is formed. This line variety has a property that is, the centers of the three planar pencils lie on the pivot line. Figure 9 (b) shows the lateral view of this configuration with three blue lines representing the projection of the pencils onto the side plane, one blue line representing the pivot line connecting all three pencil centers. Therefore, all six line in Γ intersect the pivot line, thus forming a *special complex* with order 5. By Eq.(9), the redundant constraint ν then becomes 1 and Eq.(2) yields:

$$M = 6(5-6-1) + (3\times 3 + 1\times 3) + 1 = 1 \qquad (16)$$

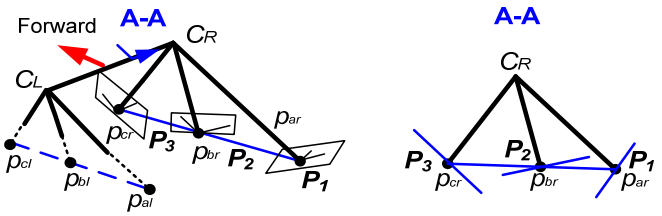

(a) 3D View (b) Lateral View

Figure 9. The Constraint Screw System of the 3-spoke SP Parallel Mechanism in 3-0 case.

3.3.2 3-1, 3-2, 3-3 contact cases:

These cases are shown in Figure 8 (b)-(d), which have more than three contact points with the ground. Note that, $p_{ar}p_{br}p_{cr}$-p_{al} and $p_{ar}p_{br}p_{cr}$-p_{cl} are of the same type; $p_{ar}p_{br}p_{cr}$-p_{al} p_{bl} and $p_{ar}p_{br}p_{cr}$-$p_{cl}p_{bl}$ are of the same type. These overconstrained configurations have similar mobility characteristics and are discussed together in this subsection. Apply Eq.(1) to these cases yields negative results as shown below:

3-1 case:

$$M = 6\times(6-8-1) + (3\times 4 + 1\times 4) = -2 \qquad (17)$$

3-2 case:

$$M = 6\times(7-10-1) + (3\times 5 + 1\times 5) = -4 \qquad (18)$$

3-3 case:

$$M = 6\times(8-12-1) + (3\times 6 + 1\times 6) = -6 \qquad (19)$$

The characteristic of zero-mobility can be correctly shown by using Eq.(2) and (4). In these configurations, the constraint screw systems are formed by at least four planar pencils. These planar pencils have no common screws (λ = 0) and typical form a line variety with order 6 unless in singularity occurs. Note that, singularity is an important part in the future research of this robot. However, the main focus in this paper is the mobility of general configurations. Apply Eq.(4) to these cases, the following results are obtained:

3-1 case:

$$\nu = 2\times 4 - 0\times 4 - 6 = 2 \qquad (20)$$

3-2 case:

$$\nu = 2\times 5 - 0\times 5 - 6 = 4 \qquad (21)$$

3-3 case:

$$\nu = 2\times 6 - 0\times 6 - 6 = 6 \qquad (22)$$

Combining Eq.(17)-(19) and Eq.(20)-(22), the zero mobility of these cases are successfully shown.

The results of mobility analysis on these cases are demonstrated in Table 3. Both conventional *Grübler* and *Kutzbach criterion* and Modified *Grübler* and *Kutzbach criterion* using reciprocal screws are adopted to obtain the correct number of d.o.f in each case.

Table 3. Mobility Analysis

Case	D.O.F
1-0	4*
1-1	2
2-0	2*
2-1	0, if no parallel spokes exist or the parallel spokes are unequal 1,if a pair of parallel spokes exist and the parallel spokes are equal
2-2	0, if two pairs of parallel spokes don't exist or the parallel spokes are unequal 1,if two pairs of parallel spoke exist and the parallel spokes are equal
3-0	1*
3-1	0
3-2	0
3-3	0

*Passive d.o.f. exist in this configuration

4. GEOMETRICAL ANALYSIS

As shown in Figure 10, the transformation from the moving platform to the body base can be described by a position vector $\mathbf{P}=\boldsymbol{OP}$, and a 3 x 3 rotation matrix ${}^{B}R_{M}$. The transforming matrix from the body coordinates, B, to the global coordinates, G, is defined as ${}^{G}R_{B}$.

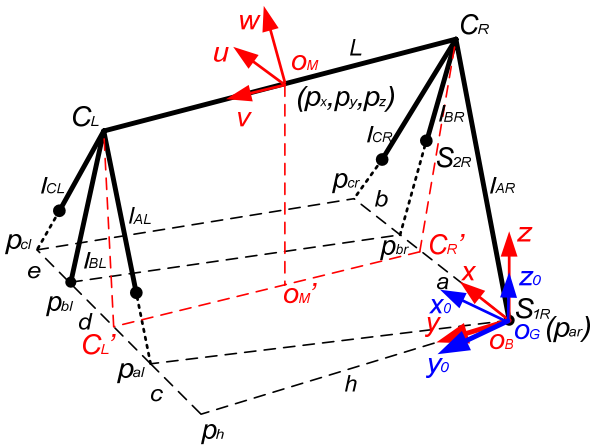

Figure 10. Geometrical Model of IMPASS.

Let **u**, **v**, and **w** be three unit vectors defined along the u, v, and w axes of the moving coordinate system M, respectively; then the rotation matrix can be expressed in terms of the direction cosines of **u**, **v**, and **w** as

$$ {}^{G}R_{B}=\begin{pmatrix} c\theta & s\theta & 0 \\ -s\theta & c\theta & 0 \\ 0 & 0 & 1 \end{pmatrix}, {}^{B}R_{M}=\begin{pmatrix} u_x & v_x & w_x \\ u_y & v_y & w_y \\ u_z & v_z & w_z \end{pmatrix}, \quad . \tag{23} $$

$$ {}^{G}R_{M}=\begin{pmatrix} u_x c\theta+u_y s\theta & v_x c\theta+v_y s\theta & w_x c\theta+w_y s\theta \\ -u_x s\theta+u_y c\theta & -v_x s\theta+v_y c\theta & -w_x s\theta+w_y c\theta \\ u_z & v_z & w_z \end{pmatrix}. $$

Here $s\theta$ and $c\theta$ stand for $\sin\theta$ and $\cos\theta$, respectively.

We note that the elements of ${}^{B}R_{M}$ must satisfy the following orthogonal conditions:

$$ \begin{aligned} u_x^2+u_y^2+u_z^2=1, v_x^2+v_y^2+v_z^2=1, \\ w_x^2+w_y^2+w_z^2=1, u_x v_x+u_y v_y+u_z v_z=0, \\ u_z w_z+u_y w_y+u_z w_z=0, v_x w_x+v_y w_y+v_z w_z=0. \end{aligned} \tag{24} $$

Let $\mathbf{b_{1R}}$, $\mathbf{b_{2R}}$, $\mathbf{b_{3R}}$, $\mathbf{g_{1R}}$, $\mathbf{g_{2R}}$, $\mathbf{g_{3R}}$, and $\mathbf{b_{1L}}$, $\mathbf{b_{2L}}$, $\mathbf{b_{3L}}$, $\mathbf{g_{1L}}$, $\mathbf{g_{2L}}$, $\mathbf{g_{3L}}$, be the position vectors of points P_{AR}, P_{BR}, P_{CR} and P_{AL}, P_{BL}, P_{CL} in the coordinate systems B and G. Then the coordinates are given by

$$ \begin{aligned} \mathbf{b_{1R}}=[0,0,0]^T, \mathbf{b_{2R}}=[a,0,0]^T, \\ \mathbf{b_{3R}}=[b,0,0]^T, \mathbf{b_{1L}}=[c,h,0]^T, \\ \mathbf{b_{2L}}=[d,h,0]^T, \mathbf{b_{3L}}=[e,h,0]^T; \\ \mathbf{g_{1R}}=[0,0,0]^T, \\ \mathbf{g_{2R}}=[ac\theta,-as\theta,0]^T, \\ \mathbf{g_{3R}}=[bc\theta,-bs\theta,0]^T, \\ \mathbf{g_{1L}}=[cc\theta+hs\theta,-cs\theta+hc\theta,0]^T, \\ \mathbf{g_{2L}}=[dc\theta+hs\theta,-ds\theta+hc\theta,0]^T, \\ \mathbf{g_{3L}}=[ec\theta+hs\theta,-es\theta+hc\theta,0]^T. \end{aligned} \tag{25} $$

Let ${}^{\mathbf{M}}\mathbf{R}$, and ${}^{\mathbf{M}}\mathbf{L}$ be the position vectors of points C_R, and C_L in the coordinate systems M. Then the coordinates of C_R, and C_L are expressed as:

$$ {}^{\mathbf{M}}\mathbf{c_R}=[0,-\frac{L}{2},0]^T, {}^{\mathbf{M}}\mathbf{c_L}=[0,\frac{L}{2},0]^T. \tag{26} $$

The position vectors $\mathbf{b_R}$, $\mathbf{b_L}$ and $\mathbf{g_R}$, $\mathbf{g_L}$ of C_R, C_L with respect to the body coordinate system B and the global coordinate system G are obtained by the following transformations:

$$ \begin{aligned} \mathbf{b_R}=\mathbf{p}+{}^{B}R_{M}\,{}^{\mathbf{M}}\mathbf{c_R}, \mathbf{b_L}=\mathbf{p}+{}^{B}R_{M}\,{}^{\mathbf{M}}\mathbf{c_L}. \\ \mathbf{g_R}={}^{G}R_{B}\mathbf{b_R}, \mathbf{g_L}={}^{G}R_{B}\mathbf{b_L}. \end{aligned} \tag{27} $$

Substituting Equations (23) and (26) into (27) yields

$$\mathbf{b_R} = \begin{bmatrix} p_x - \frac{L}{2}v_x \\ p_y - \frac{L}{2}v_y \\ p_z - \frac{L}{2}v_z \end{bmatrix}, \mathbf{b_L} = \begin{bmatrix} p_x + \frac{L}{2}v_x \\ p_y + \frac{L}{2}v_y \\ p_z + \frac{L}{2}v_z \end{bmatrix};$$

$$\mathbf{g_R} = \begin{bmatrix} (p_x - \frac{L}{2}v_x)c\theta + (p_y - \frac{L}{2}v_y)s\theta \\ -(p_x - \frac{L}{2}v_x)s\theta + (p_y - \frac{L}{2}v_y)c\theta \\ p_z - \frac{L}{2}v_z \end{bmatrix},$$

$$\mathbf{g_L} = \begin{bmatrix} (p_x + \frac{L}{2}v_x)c\theta + (p_y + \frac{L}{2}v_y)s\theta \\ -(p_x + \frac{L}{2}v_x)s\theta + (p_y + \frac{L}{2}v_y)c\theta \\ p_z + \frac{L}{2}v_z \end{bmatrix}. \quad (28)$$

4.1 Constraints Analysis:

Since the axle is always perpendicular to both spokes, $C_R\,C_L$ is also perpendicular to *x*-axis. Then Equation (24) becomes

$$\begin{aligned} u_x = 1, u_y = 0, u_z = 0, \\ v_x = 0, w_x = 0, v_y^2 + v_z^2 = 1, \\ w_y^2 + w_z^2 = 1, v_y w_y + v_z w_z = 0, \end{aligned} \quad (29)$$

and the following constraints can be obtained:

$$p_y = \frac{h}{2}, v_y = \frac{h}{L}. \quad (30)$$

As we know, the left wheel spokes are parallel to the corresponding right wheel spokes, so the following equation is defined:

$$\frac{l_{AL}}{l_{AR}} = \frac{l_{BL}}{l_{BR}} = \frac{l_{CL}}{l_{CR}} = \frac{e-d}{b-a} = \frac{d-c}{a} = \frac{\mathbf{b}_{Lz}}{\mathbf{b}_{Rz}} = R, \quad (31)$$

Since $\beta = 60°$, according to the triangle geometry, the following equations are derived:

$$\begin{aligned} a^2 &= l_{AR}^2 + l_{BR}^2 - l_{AR}l_{BR}, \\ b^2 &= l_{AR}^2 + l_{CR}^2 - l_{AR}l_{CR}, \\ (b-a)^2 &= l_{BR}^2 + l_{CR}^2 - l_{BR}l_{CR}. \end{aligned} \quad (32)$$

4.2 Effective Spokes Lengths:

The effective spoke length, l_{AR}, l_{BR}, l_{CR} and l_{AL}, l_{BL}, l_{CR} shown in Figure 10, is given by

$$\begin{aligned} l_{iR}^2 &= [q_R - a_{iR}]^T[q_R - a_{iR}], \\ l_{iL}^2 &= [q_L - a_{iL}]^T[q_L - a_{iL}]. \end{aligned} \quad \text{for i=A,B,C} \quad (33)$$

Substituting Equation (25), (28), (30) through (31) into (33), the right effective spoke lengths become:

$$\begin{aligned} l_{AR}^2 &= p_x^2 + p_z^2 - Lp_z v_z + \frac{L^2}{4}v_z^2, \\ l_{BR}^2 &= p_x^2 + p_z^2 - Lp_z v_z + \frac{L^2}{4}v_z^2 - 2ap_x + a^2, \\ l_{CR}^2 &= p_x^2 + p_z^2 - Lp_z v_z + \frac{L^2}{4}v_z^2 - 2bp_x + b^2. \end{aligned} \quad (34)$$

The left effective spoke lengths yield:

$$\begin{aligned} l_{AL}^2 &= p_x^2 + p_z^2 + Lv_z p_z + \frac{L^2}{4}v_z^2 - 2cp_x + c^2, \\ l_{BL}^2 &= p_x^2 + p_z^2 + Lv_z p_z + \frac{L^2}{4}v_z^2 - 2dp_x + d^2, \\ l_{CL}^2 &= p_x^2 + p_z^2 + Lv_z p_z + \frac{L^2}{4}v_z^2 - 2ep_x + e^2. \end{aligned} \quad (35)$$

As *R=1*, the kinematics analysis of IMPASS becomes a 2D planar problem. Besides the geometrical analysis mentioned above, the following extra constraints yield:

$$R = 1, c = 0, d = a, v_y = 1, h = L, p_y = \frac{L}{2}. \quad (36)$$

5. CONCLUSIONS AND FUTURE RESEARCH

This paper presents a novel Intelligent Mobility Platform with Active Spoke System (IMPASS). Based on system modeling and definition, the mobility and geometrical analysis of IMPASS is studied. The variable topology structures of the robot are classified into difference cases due to various schemes of ground contact points. In order to derive the correct number of d.o.f. for each case, two types of *Grübler* and *Kutzbach criterion*, conventional criterion and modified criterion using reciprocal screws, are adopted. It shows that the Modified *Grübler* and *Kutzbach criterion* can successfully identify the d.o.f. of overconstrained configurations under which the conventional criterion fails. The process of the mobility analysis on the overconstrained cases of this robot is simplified with the assistance of *line geometry*.

The results obtained from the mobility analysis and the geometrical constraint equations lay the foundation for the future research on the kinematics of IMPASS, such as inverse, forward position analysis, Jacobian analysis, singularity and etc. They also provide theoretical background to the dynamics analysis and motion planning strategy.

6. ACKNOWLEGMENTS

The support of the National Science Foundation under Grant No. 0535012 is gratefully acknowledged. The authors would also like to thank Shawn Kimmel and his senior design project

team for their contribution in the development of IMPASS prototypes.

REFERENCES

[1] M. Hiller, D. Germann, J.A Morgado de Gois, "Design and Control of a Quadruped Robot Walking in Unstructured Terrain'', Proceedings of the 2004 IEEE Intern. Conf. on Control Applications, pp. 916 -- 921, vol. 2, Taipei, 2004.

[2] robotics.jpl.nasa.gov/systems/systemImages.cfm?System =11

[3] Kawee Suwannasit and Sathaporn Laksanacharoen, "A Bio-Inspired Hybrid Leg-Wheel Robot", TENCON 2004. 2004 IEEE Region 10 Conference, pp.495-497.

[4] Benjamin E. Shores and Mark A. Minor, "Design, Kinematic Analysis, and Quasi-Steady Control of a Morphic Rolling Disk Biped Climbing Robot", Proceedings of the 2005 IEEE International Conference on Robotics and Automation, Barcelona, Spain, April 2005.

[5] Drenner, A., Burt, I., Kratochvil, B., Nelson, B., Papanikolopoulos, N., and Yesin, K. B., "Cocmunication and Mobility Enhancements to the Scout Robot," Proceedings of the 2003 IEEE/RSJ International Conference on Intelligent Robots and Systems, Lausanne, Switzerland, Oct. 2002.

[6] Drenner, A., Burt, I., Dahlin, T., Kratochvil, B., McMillen, C., Nelson, B., Papanikolopoulos, N., Rybski, P. E., Stubbs, K., Waletzko, D., Yesin, K. B., "Mobility Enhancements to the Scout Robot Platform," Proceedings of the 2002 IEEE International Conference on Robots and Automation, Washington DC, USA, May 2002.

[7] Saranli, U., Buehler, M., and Koditschek, D.E. "RHex: A Simple and Highly Mobile Hexapod Robot," International Journal of Robotics Research 20, July 2001, pp. 616-631.

[8] Allen, T., Quinn, R. D., Bachmann, R. J., Ritzman, R. E., "Abstracted Biological Principles Applied with Reduced Actuation Improve Mobility of Legged Vehicles," Proceedings of the 2003 IEEE/RSJ International Conference on Intelligent Robots and Systems, Las Vegas, NV, Oct. 2003, pp. 1370-1375.

[9] Goeken, M. and Kempf, M., 1999, "Microstructural Properties of Superalloys Investigated by Nanoindentations in an Atomic Force Microscope", *Acta Materialia*, Vol.47 (3), pp. 1043-1052.

[10] Laney, D. and Hong, D.W.,"Kinematic Analysis of a Novel Rimless Wheel with Independently Actuated Spokes", 29th ASME Mechanisms and Robotics Conference, Long Beach, California, September 24-28, 2005.

[11] Hong. D.W. and Laney, D., "Preliminary Design and Kinematic Analysis of a Mobility Platform with Two Actuated Spoke Wheels", US-Korea Conference on Science, Technology and Entrepreneurship (UKC 2006), Mechanical Engineering & Robotics Symposium, Teaneck, New Jersey, August 10-13, 2006.

[12] Laney, D. and Hong, D.W., "Three-Dimensional Kinematic Analysis of the Actuated Spoke Wheel Robot". 30th ASME Mechanisms and Robotics Conference, Philadelphia, Pennsylvania, September 10-13, 2006.

[13] Wohlhart,K. "Kinematotropic Linkages," Recent Advances in Robot Kinematics, Kluwer Academic, Dordrecht, The Netherlands, pp.359-368, 1996

[14] Dai, J. S., Jones, J.R., "Mobility in Metamorphic Mechanisms of Foldable/Erectable Kinds," Proceedings of ASME DETC, Atlanta, GA, September 13-16, 1999

[15] Tsai, Lung-Wen, "Robot Analysis, the Mechanics of Serial and Parallel Manipulators," John Wiley & Sons, Inc., 1999

[16] Tsai, Lung-Wen, Stamper,R., "A Parallel Manipulator with Only Translational Degrees of Freedom," Proceedings of ASME DETC, Irvine, CA, 1996

[17] O. Bottema, "On Gruebler's Formulae for Mechanisms," Applied Scientific Research A2,162-164, 1950

[18] F. Freudenstein, R. Alizade, "On the Degree of Freedom of Mechanisms with Variable General Constraint", Proceedings of the Fourth World Congress on the Theory of Machines and Mechanisms, London: The Institution of Mechanical Engineers, 51-55, 1975

[19] Huang, Z., Ge, Q.J., "A Simple Method for Mobility Analysis Using Reciprocal Screws", 30th ASME Mechanisms and Robotics Conference, Philadelphia, Pennsylvania, September 10-13, 2006.

[20] Dai, J.S., Huang, Z., Lipkin, H., "Mobility of Overconstrained Parallel Mechanisms," Journal of Mechanical Design, Vol.128, January 2006

[21] Dandurand, A., "The rigidity of compound spatial grid," Structural Topology, Vol.10, pp 41-55, 1984.

[22] Pottmann, H., Peternell, M., Ravani, B., "An Introduction to Line Geometry with Applications," Computer-Aided Design, Vol.31, pp 3-16, 1999

[23] Ren, P., Wang, Y., Hong, D.W., "Three-dimensional Kinematic Analysis of a Two Actuated Spoke Wheel Robot Based on its Equivalency to a Serial Manipulator," 32nd ASME Mechanisms and Robotics Conference, August 3-6, 2008, Brooklyn, New York, USA

